Deconvolving PSFs for A Better Motion Deblurring using Multiple Images

Xiang Zhu[1]⋆, Filip Šroubek[2], and Peyman Milanfar[1]

[1] E.E. Department, UC Santa Cruz,
1156 High St., Santa Cruz, CA 95064, USA
[2] UTIA, Academy of Sciences of the Czech Republic
182 08 Prague, Czech Republic

Abstract. Blind deconvolution of motion blur is hard, but it can be made easier if multiple images are available. This observation, and an algorithm using two differently-blurred images of a scene are the subject of this paper. While this idea is not new, existing methods have so far not delivered very practical results. In practice, the PSFs corresponding to the two given images are estimated and assumed to be close to the latent motion blurs. But in actual fact, these estimated blurs are often far from the truth, for a simple reason: They often share a common, and unidentified PSF that goes unaccounted for. That is, the estimated PSFs are themselves "blurry". While this can be due to any number of other blur sources including shallow depth of field, out of focus, lens aberrations, diffraction effects, and the like, it is also a mathematical artifact of the ill-posedness of the deconvolution problem. In this paper, instead of estimating the PSFs directly and only once from the observed images, we first generate a rough estimate of the PSFs using a robust multichannel deconvolution algorithm, and then "deconvolve the PSFs" to refine the outputs. Simulated and real data experiments show that this strategy works quite well for motion blurred images, producing state of the art results.

Key words: Blind deconvolution, motion blur, PSF.

1 Introduction

Motion blur caused by camera shake is one of the major reasons for low quality in imaging. Strictly speaking, the point-spread-function (PSF) of motion blur at a given point on an image is related to the motion type, the position and the depth. Yet in general, it is commonly modeled globally or locally as a shift-invariant convolution process:
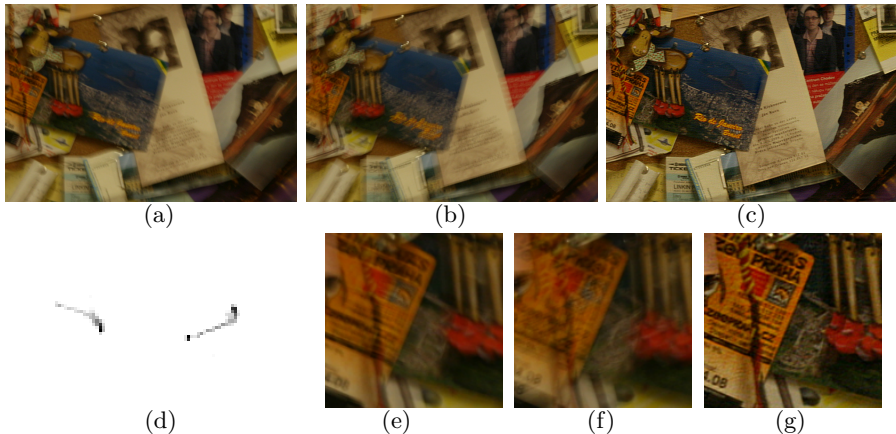
$$g = u \otimes h + n \tag{1}$$

Fig. 1. Real image blind deconvolution example using the proposed algorithm. (a)-(b) input blurry images. (c) deblurred image. (d) estimated PSFs. (e)-(g) zoomed (a)-(c).

where g and u represent the observed image and the latent sharp image, respectively; h is the blur PSF; n denotes additive noise, and $\otimes$ is the convolution operator. Recovering both u and h from a single observed image is the long-studied blind deconvolution problem. This is a highly ill-posed problem for a variety of reasons. We concentrate in this paper on one such reason, which goes often neglected. Namely, consider s as an arbitrary function which has a convolution inverse:

$$s \otimes s^{-1} = \delta, \qquad (2)$$

we can see that any pair $< \hat{u}, \hat{h} >$ could be a solution to (1) if

$$\hat{u} = u \otimes s^{-1}; \ \ \hat{h} = h \otimes s. \qquad (3)$$

To pick a solution that is more like the latent one, prior knowledge based on, say, natural image statistics is required. It has been found that natural image gradients are usually distributed through "heavy-tailed" functions, where the heavy-tail corresponds to high-valued derivatives of the salient structures (e.g. edges) of image content [1]. In [2, 3] sparsity-based regularization terms are employed to constrain the derivatives of the estimate $\hat{u}$. In [4] Joshi et al. predict sharp edges using edge profiles and estimate the blur kernel from the predicted edges. Cho et al. analyze the observation on edges and reconstruct the motion kernel using the Radon transform [5]. Unfortunately, if the blurry observation does not contain salient edges or textures most single-image blind deconvolution approaches can fail in the presence of small amounts of noise.

It has been known that the ill-posed nature of blind deconvolution can be remedied if multiple observations $\{g_i\}$ of the same scene u are available:

$$g_i = u \otimes h_i + n_i \ , \ i = 1, 2, \cdots \qquad (4)$$

In practice, there are many situations where we can get multiple images with different motion PSFs, such as burst-mode photography or video capture. Li et al. developed a camera system capable of capturing two images simultaneously with two different shaking blur PSFs perpendicular to each other [6]. For these cases *multichannel blind deconvolution* algorithms are needed. Harikumar et al. proposed an algorithm that first estimates the blur kernels using eigenvalue analysis of a special matrix constructed from the input images, and then restores the latent image using a standard non-blind deconvolution method [7]. Their estimation is based on the following relation:

$$g_1 \otimes h_2 = g_2 \otimes h_1 \qquad (5)$$

It is shown that perfect recovery of the PSFs requires *noise-free* images and channel coprimeness, i.e. a scalar constant is the only common factor of the blur PSFs. In [8] Giannakis et al. developed another algorithm finding a restoration filter-bank based on Bezout's identity of coprime polynomials. Both methods are highly sensitive to noise. Rav-Acha et al. developed a bi-channel deconvolution approach for motion deblurring, which estimates the PSFs in a way similar to [7] and meanwhile keeps the sparsity of each PSF by modeling it as a directed line [9]. However, this model is too simple and cannot deal with real camera shake. In [10] Šroubek et al. proposed a method where both the image u and the blur PSFs $\{h_i\}$ are estimated simultaneously by minimizing an energy function including a fidelity term, an l_1 norm regularizer on image gradients, and a multi-channel PSF regularizer based on (5). Noise sensitivity is nicely mitigated in this algorithm, and it can handle large PSFs without too much computational cost. However, because the exact size of the blur kernel is unknown, the ill-posedness still persists. Namely, as alluded to earlier, the estimated PSFs can be represented as convolutions between the latent PSFs and a common spurious kernel s as follows:

$$\hat{h}_i = h_i \otimes s \qquad (6)$$

since the relationship (5) still holds with s:

$$g_1 \otimes h_2 \otimes s = g_2 \otimes h_1 \otimes s. \qquad (7)$$

As we will show in Section 2, when the noise level is high, this common kernel s would make $\hat{h}_i$ blurry and cause artifacts (such as ringing) in the output $\hat{u}$. In fact, Most multichannel deconvolution algorithms utilizing the relation (5) would more or less suffer from such "hidden" blur in their PSF estimation. However, This common problem has seldom been discussed before.

To further improve the estimation accuracy on both u and $\{h_i\}$, a new multichannel deblurring strategy is proposed in this paper based on the idea of PSF refinement, or "deblurring the (estimated) blur kernels". First, a preliminary estimate of the PSFs is obtained using an algorithm similar to [10]. Next, we refine the estimate by removing the common factor s through a multi-channel deconvolution procedure. Both steps are formulated as constrained optimization problems. Augmented Lagrangian method (ALM) and iteratively re-weighted

least square (IRLS) are employed for the optimization. Finally, with the high-fidelity estimates of the blur kernels, the latent image is calculated through a standard non-blind deconvolution step. This paper is organized as follows. Section 2 gives a rough description of the preliminary PSF estimation method. Section 3 discusses the blur kernel deconvolution problem. Simulated and real image deblurring experiments are illustrated in Section 4 to show the algorithm performance, and Section 5 concludes this paper.

2   Preliminary PSF Estimation

While the general approach we present is applicable when multiple blurry frames are given, for simplicity, we consider only two observations g_1 and g_2. Let $\hat{h}_1$ and $\hat{h}_2$ be estimates of the original unknown PSFs h_1 and h_2, respectively. The multichannel PSF estimation of Harikumar [7] is based on the relation, that if $\hat{h}_i = h_i$, then

$$g_2 \otimes \hat{h}_1 - g_1 \otimes \hat{h}_2 \sim \epsilon \,, \qquad (8)$$

where ϵ is an error term proportional to noise variables n_1 and n_2. In the noiseless case $(n_i = 0)$, $\epsilon = 0$. In the case of AWGN (additive white Gaussian noise, $n_i \sim N(0, \sigma^2)$), $\epsilon \sim N(0, \Sigma)$, where[1] $\Sigma = \sigma^2(\mathbf{cov}(h_1) + \mathbf{cov}(h_2))$. Relation (8) can be proved by simple substitution for g_i from (4). If more than two observed images are available, we take all possible pairs and write a similar equation for each. We now show that this relation is an effective means of estimating PSFs directly from the observed images.

Using the vector-matrix notation, we can rewrite (8) as $[\mathbf{G}_2, -\mathbf{G}_1]\mathbf{h} \sim \epsilon$, where $\mathbf{h} = [\mathbf{h}_1^T, \mathbf{h}_2^T]^T$ represent the vectorized blur kernels and $\mathbf{G}_i$ the convolution matrix based on g_i. The maximum-likelihood (ML) estimation of the blur kernels for AWGN is equivalent to $\hat{\mathbf{h}} = \arg\min_{\mathbf{h}} \|\epsilon\|^2$ with a constraint, i.e.,

$$\hat{h} = \arg\min_{\mathbf{h}} \mathbf{h}^T [\mathbf{G}_2, -\mathbf{G}_1]^T \Sigma^{-1} [\mathbf{G}_2, -\mathbf{G}_1]\mathbf{h} \quad \text{s.t.} \quad \forall i \sum_j h_i(j) = 1 \,. \quad (9)$$

The constraint is necessary to avoid the trivial solution of $\hat{h}_i = 0$. Note that Σ depends not only on the noise variance but also on the covariance matrices of h_i's, which are not known a priori. For low noise levels, Σ can be neglected. For higher noise levels (SNR $\leq$ 30dB) it is demonstrated in [10] that by simple linear transformation Σ can be partially eliminated as well. The main shortcoming of the ML estimator is the fact that correct PSFs convolved with an arbitrary spurious kernel $(\hat{h}_i = s \otimes h_i)$ are also ML estimates. In other words, correct PSFs and their commonly blurred versions are equally probable. One way to avoid this indeterminacy of solution is to constrain the maximum size of the estimated PSFs, so that the only allowable spurious kernel would be a scalar. However, this requires prior knowledge of the size of the original PSFs, which is generally not available.

---

[1] $\mathbf{cov}(h) = \mathbf{H}\mathbf{H}^T$, where $\mathbf{H}$ is the convolution matrix based on h.

Since image u and h_i's are related through (4), prior knowledge on u can be used to implicitly constrain the solution of h_i's. We also include a positivity constraint on PSFs and use the objective function in (9) as a regularization term. Let $A(\{h_i\}) = \|g_2 \otimes h_1 - g_1 \otimes h_2\|^2$ and $B(u)$ be some convex image regularization term, such as Total Variation [11]. Then we minimize an objective function

$$E(u, \{h_i\}) = \sum_i \|h_i \otimes u - g_i\|^2 + \alpha A(\{h_i\}) + \beta B(u) \qquad (10)$$

with respect to the image u and with respect to the blur kernels h_i's in an alternating manner, and subject to $\forall i \; h_i > 0$. Weights α and β are parameters depending on the noise level. Since the minimization is constrained and edge-preserving priors $B(u)$ are based on the ℓ_1 norm, a fast converging ALM is applied, which guarantees convergence for this type of problems [10].

3   PSF Refinement

Though the estimation approach in Section 2 provides better estimates than the simple ML estimator, it still suffers from indeterminacy of solutions. This is primarily noticeable in the case of sparse PSFs, such as motion blurs, and in the presence of strong noise. Consider plugging the estimates $\hat{h}_i = s \otimes h_i$ into the regularization term $A(\{h_i\})$:

$$\begin{aligned} A(\{\hat{h}_i\}) &= \|g_2 \otimes h_1 \otimes s - g_1 \otimes h_2 \otimes s\|^2 \\ &= \| (n_2 \otimes h_1 - n_1 \otimes h_2) \otimes s\|^2 \end{aligned} \qquad (11)$$

Minimizing this term tends to select the kernel s that performs like a low-pass filter, which would inevitably lead to blurry PSFs and ringing artifacts in the output image. A simulated example is given in Fig. 2-3, where as the noise level increases the estimated PSFs become more and more blurry. In this section, we propose a way to address this problem.

Since s is a common kernel among the estimates, it can be deconvolved again through a multichannel blind deconvolution procedure. The degradation model for the output PSFs in Section 2 can be written as

$$h_i^0 = h_i \otimes s + \varepsilon_i. \qquad (12)$$

where in this section $\{h_i^0\}$ denotes the blurry PSFs estimated from the previous step in Section 2. Since motion-caused PSFs describe the path of camera motion, they tend to be sparse. So a sparsity-based regularization term should be considered. Besides, we add positivity constraints for both s and $\{h_i\}$, and the PSF refinement can thus be treated as optimizing the following objective function:

$$\begin{aligned} E(s, \{h_i\}) = &\sum_i \|s \otimes h_i - h_i^0\|^2 + \delta\Psi(s) + \\ &\delta\Psi(\{h_i\}) + \gamma\Phi_p(\{h_i\}) \end{aligned} \qquad (13)$$
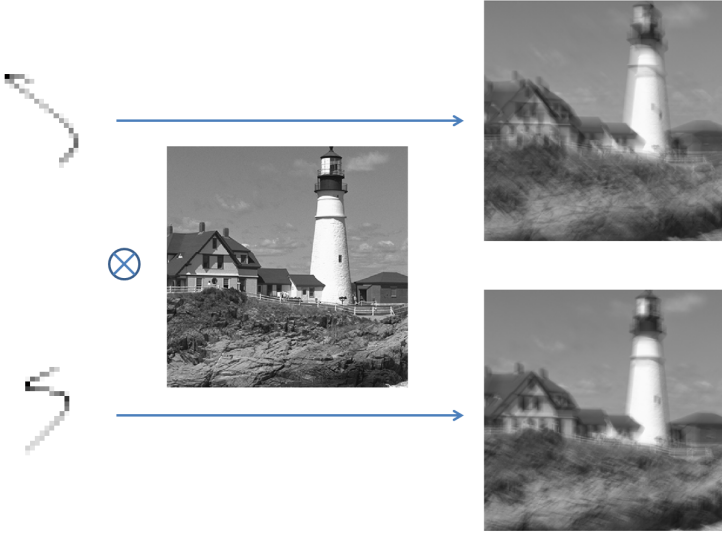
Fig. 2. Simulated blurry images using model (4).

where $\Psi(\cdot)$ denotes the positivity constraint:

$$\Psi(h) = \sum_{\mathbf{x}} \psi(h(\mathbf{x})), \; \psi(t) = \begin{cases} t & \text{if } t \geq 0 \\ +\infty & \text{otherwise} \end{cases} \tag{14}$$

and $\Phi_p(\cdot)$ represents an l_p norm regularizer, which can be written in vector form:

$$\Phi_p(\{h_i\}) = \|\mathbf{h}\|_p^p \tag{15}$$

where again $\mathbf{h}$ represents a stacked column vector for $\{h_i\}$. The sparsity of the PSFs can be preserved when $p \in [0, 1]$ [3]. However, in general for $p < 1$ the cost function is no longer convex, which complicates the optimization. To address this problem, we use an iterative re-weighted least square (IRLS) method that describes the regularization term through a weighted least square form:

$$\Phi_{\mathbf{W}}(\mathbf{h}) = \mathbf{h}^T \mathbf{W} \mathbf{h} \tag{16}$$

where the diagonal weight matrix $\mathbf{W}$ is updated during the iteration minimizing (13). For example, in the j-th iteration when the estimate $\mathbf{h}^{j-1}$ is available, we have

$$\mathbf{W}^{j-1} = \text{diag}(\{w_{i,\mathbf{x}}^{-1}\}) \tag{17}$$

where $w_{i,\mathbf{x}} = |h_i^{j-1}(\mathbf{x})|^{2-p} + \eta$. η is a small constant to prevent division by zero. As the iteration converges: $\mathbf{h}_i^{j-1} \to \mathbf{h}_i^j$, the regularization term becomes:

$$\mathbf{h}^{jT} \mathbf{W}^{j-1} \mathbf{h}^j \to \mathbf{h}^{jT} \mathbf{W}^j \mathbf{h}^j \approx \|\mathbf{h}^j\|_p^p \tag{18}$$
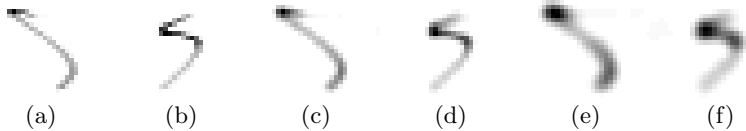
Fig. 3. PSFs estimated from the simulated blurry image pairs (see Fig. 2) with different levels of AWGN using the blind deconvolution algorithm described in Section 2. (a), (b): results of noise level $\sigma = 0$. (c), (d): results of noise level $\sigma = 1$. (e), (f): results of noise level $\sigma = 5$.

which is equivalent to an l_p norm regularizer.

Minimizing (13) is achieved through a procedure that alternates minimizing s and $\{h_i\}$. The procedure is described in Algorithm 1.

Algorithm 1

---

1. Set $j = 0$, and initialize s^j.
2. $\mathbf{h}^{j+1} = \arg\min_{\mathbf{h}} \sum_i \|s^j \otimes h_i - h_i^0\|^2 + \delta\Psi(\mathbf{h}) + \gamma\mathbf{h}^T\mathbf{W}^j\mathbf{h}$.
3. $s^{j+1} = \arg\min_s \sum_i \|s \otimes h_i^{j+1} - h_i^0\|^2 + \delta\Psi(s)$.
4. $j \leftarrow j + 1$.
5. End the algorithm if stopping criterion is satisfied, otherwise go to Step 2.

Because the positivity constraint is not quadratic, solving both Step 2 and 3 in Algorithm 1 directly is not trivial. Split Bregman method (or ALM) is implemented here. Take Step 2 for example (and Step 3 can be solved in a similar way), which minimizes:

$$\min_{\{h_i\}} \sum_i \|s^j \otimes h_i - h_i^0\|^2 + \delta\Psi(h_i) + \gamma\mathbf{h}^T\mathbf{W}^j\mathbf{h}. \tag{19}$$

This is equivalent to a constraint minimization problem:

$$\min_{\mathbf{h},\mathbf{v}} \|\mathbf{S}^j\mathbf{h} - \mathbf{h}^0\|^2 + \gamma\mathbf{h}^T\mathbf{W}^j\mathbf{h} + \delta\Psi(\mathbf{v}) \\ \text{s.t. } \mathbf{v} = \mathbf{h} \tag{20}$$

where $\mathbf{S}^j$ denotes a convolution matrix of s^j. The split Bregman tackles this problem by considering a function:

$$\mathcal{L}(\mathbf{h}, \mathbf{w}) = \|\mathbf{S}^j\mathbf{h} - \mathbf{h}^0\|^2 + \gamma\mathbf{h}^T\mathbf{W}^j\mathbf{h} + \delta\Psi(\mathbf{v}) + \lambda\|\mathbf{h} - \mathbf{v} - \mathbf{b}\|^2 \tag{21}$$

and solve it with the following iterative algorithm:

Once the refined PSFs $\{\hat{h}_i\}$ are available, the deblurred image can be estimated by minimizing the following cost function:

$$E(u) = \sum_i \|\hat{h}_i \otimes u - g_i\|^2 + \beta B(u) \tag{22}$$

Algorithm 2

---

1. Set $\mathbf{v}^1 = \mathbf{b}^1 = 0$ and $n = 0$.
2. $\mathbf{h}^{n+1} = \arg\min_{\mathbf{h}} \mathcal{L}(\mathbf{h}, \mathbf{v}^n) \Longleftrightarrow$
$\left[\mathbf{S}^{jT}\mathbf{S}^j + \gamma\mathbf{W}^j + \lambda\mathbf{I}\right]\mathbf{h}^{n+1} = \mathbf{S}^{jT}\mathbf{h}^0 + \lambda\left(\mathbf{v}^n + \mathbf{b}^n\right)$
3. $\mathbf{v}^{n+1} = \arg\min_{\mathbf{v}} \mathcal{L}(\mathbf{h}^{n+1}, \mathbf{v}) \Longleftrightarrow$
$\mathbf{v}^{n+1}[\mathbf{x}] = \max\left((\mathbf{h}^{n+1} - \mathbf{b}^j)[\mathbf{x}] - \frac{\delta}{2\lambda}, 0\right)$
4. $\mathbf{b}^{n+1} = \mathbf{b}^n - \mathbf{h}^{n+1} + \mathbf{v}^{n+1}$.
5. End the algorithm if stopping criterion is satisfied, otherwise set $n \leftarrow n + 1$ and go to Step 2.

---

where in our implementation $B(u)$ is selected as a gradient-based TV regularizer.

4   Experimental results

In this section we test the performance of the proposed method compared with other blind deconvolution algorithms. Firstly simulated experiments are carried out where the latent image is available and the restoration performance can be quantitatively measured using full-reference image quality metrics such as mean squared error (MSE). We simulated a set of images according to the model (4) with different signal-to-noise-ratio: SNR $= 34, 24, 20, 17, 14$dB. The original image and the latent PSFs are illustrated in Fig. 2. State-of-the-art single-image blind deconvolution methods [12] and [13] are also implemented for comparison.
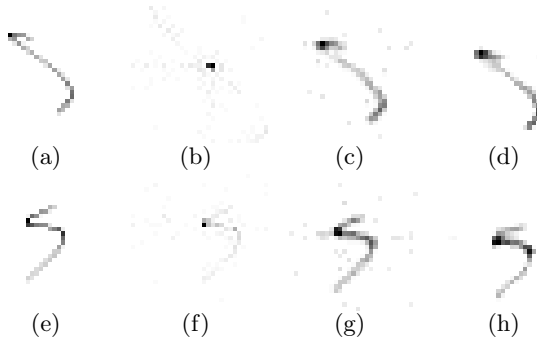

(a)   (b)   (c)   (d)

(e)   (f)   (g)   (h)

Fig. 4. PSFs for the simulated experiments with SNR $= 17$dB. (a), (e) latent PSFs. (b), (f) output PSFs of [13]. (c), (g) output PSFs of [12]. (d), (h) proposed outputs.

Fig. 4 illustrates examples of the PSFs estimated from the image pair with SNR $= 17$dB, where noise effects can be observed. Xu et al.'s method [12] captured the basic shape of the latent PSFs, but these are somewhat blurry PSFs themselves, and contaminated with strong noise, which leads to artifacts in the output image (see Fig. 5 (d)). Similar noise effect can be observed in
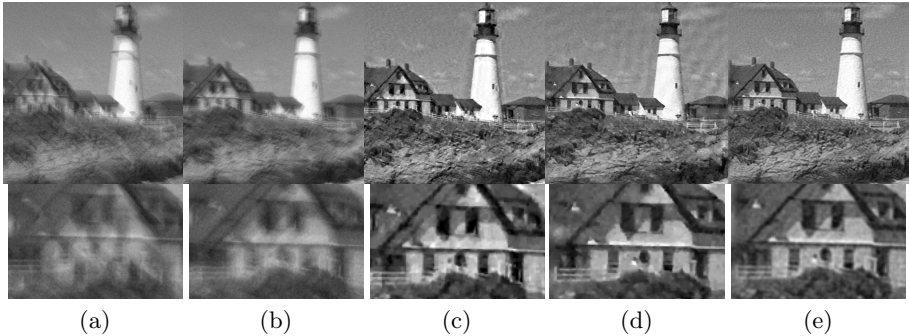
(a)   (b)   (c)   (d)   (e)

Fig. 5. Simulated experiments with SNR = 17dB. (a)-(b) input images. (c) output of [13] using the image (b). (d) output of [12] using image (a). (e) the proposed output.

the output of [13] for the second PSF (Fig. 4 (f)), while this method failed in estimating the first one (Fig. 4 (b)). The proposed algorithm provides PSFs that are much cleaner and sharper (Fig. 4 (d), (h)), and also gives an output image with lower MSE compared with the other two. The MSE values for the deblurred images using different algorithms are given in Table 1.

Table 1. Performance of the deconvolution approaches evaluated in MSE.

SNR	34dB	24dB	20dB	17dB	14dB
Proposed	**95.45**	**121.07**	**152.85**	**183.17**	**233.70**
[12] (h_1)	132.76	139.69	189.48	240.02	304.54
[12] (h_2)	132.69	160.38	187.60	198.50	339.94
[13] (h_1)	814.55	816.15	823.04	850.10	998.45
[13] (h_2)	234.53	239.21	259.17	312.39	434.68

Additional tests using real images with large blur kernels are given in Fig. 1 and Fig. 6-7, where it can be seen that the proposed method successfully removed motion blur, and the estimated PSFs are clean and describe the motion path quite well. In Fig. 6, the outputs of the preliminary deconvolution step described in Section 2 are also provided in (c) and (g). Ringing artifacts caused by the spurious kernel can be easily observed, which makes the letters in the image content hard to recognize. However, after the PSF refinement these letters are more distinct (see (h) in Fig. 6). In Fig. 7 we compare our method with a state-of-the-art dual image deblurring method [14][2]. Both completely removed the motion blur, and generated PSFs that are sharp and clean. Details on the image of the map are successfully recovered by the two methods.

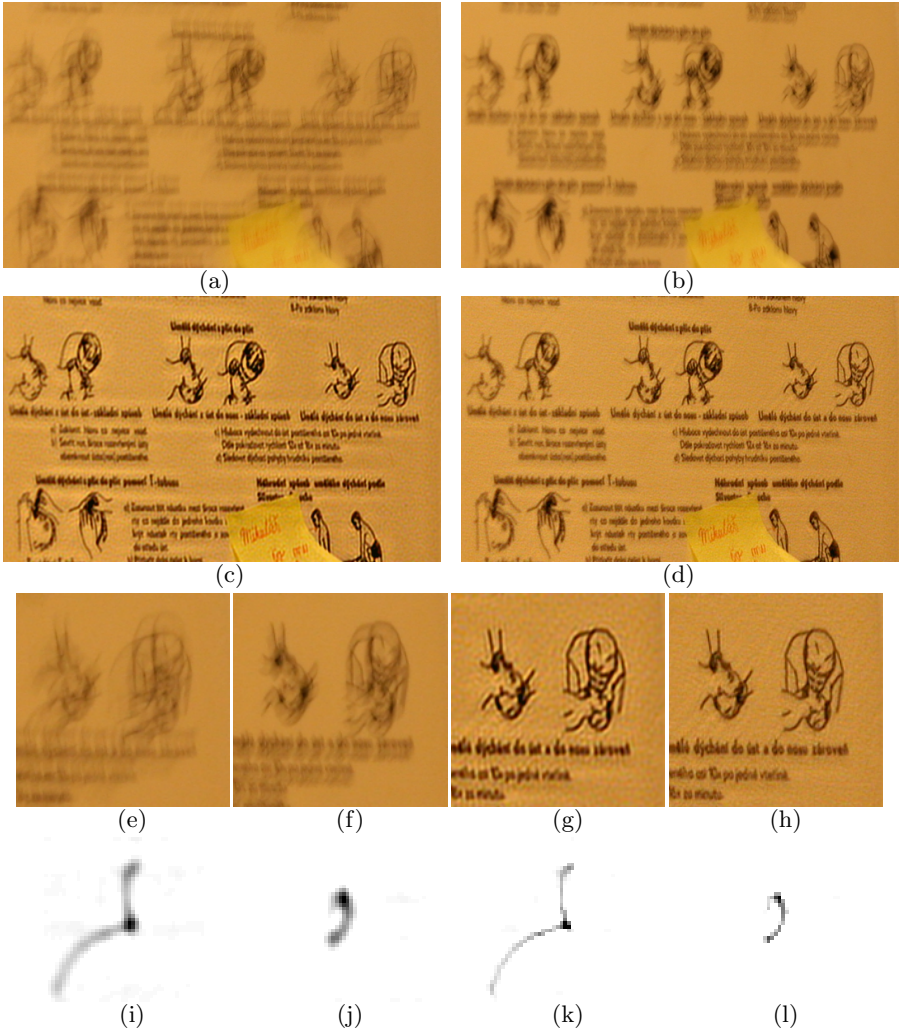[2] The test images are extracted from the paper [14].

Fig. 6. Real image blind deconvolution example using the proposed algorithm. (a)-(b) input blurry images. (c) deblurred image only using the preliminary deconvolution step described in Section 2. (d) proposed output. (e)-(h) zoomed (a)-(d). (i)-(j) estimated PSFs using the preliminary deconvolution step described in Section 2. (k)-(l) refined PSFs.

5   Conclusions and Discussions

A new algorithm for motion deblurring using multiple images is described in this paper. This approach first roughly estimates the PSFs by minimizing a cost function incorporating a multichannel PSF regularization term and an l_1 norm-based image sparsity regularizer. This step generates reasonable, but blurry PSFs,
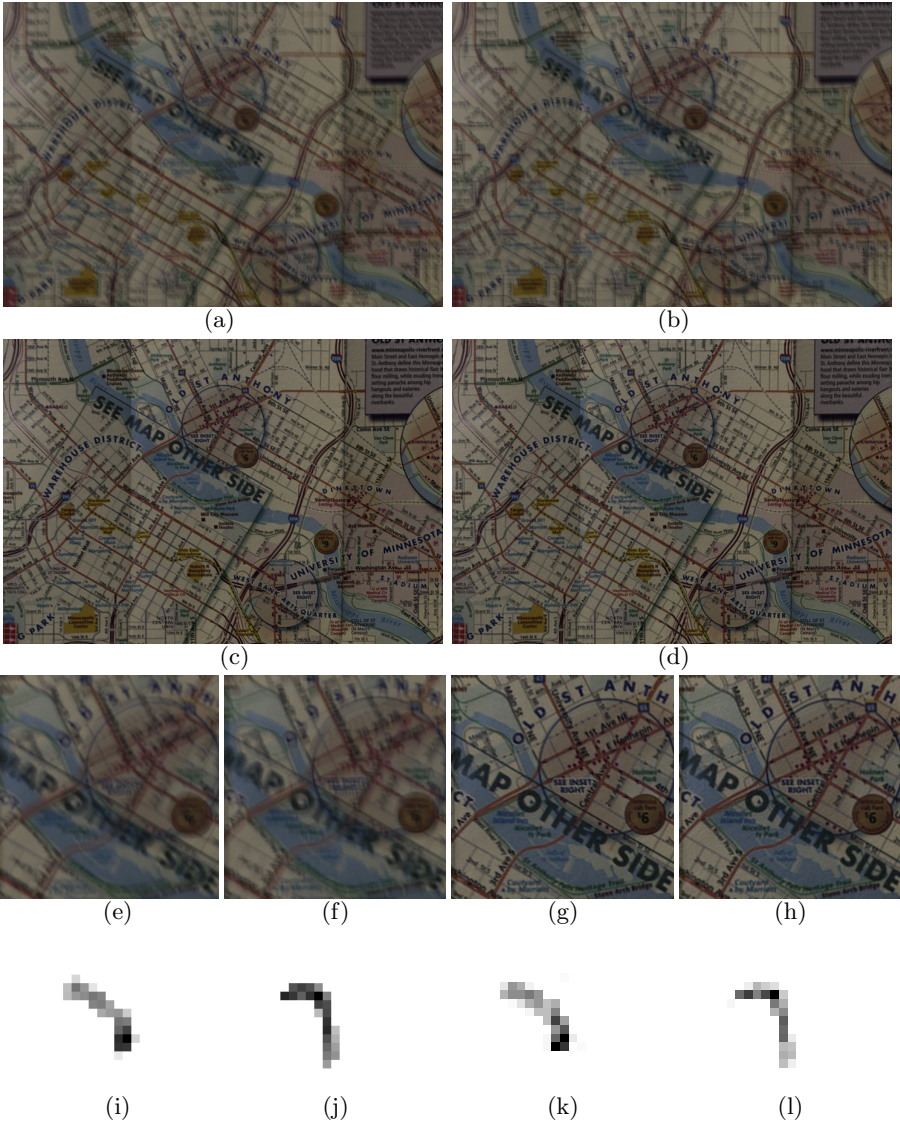
Fig. 7. Real image blind deconvolution example using the proposed algorithm and [14]. (a)-(b) input blurry images. (c) deblurred image using [14]. (d) proposed output. (e)-(h) zoomed (a)-(d). (i)-(j) estimated PSFs using [14]. (k)-(l) estimated PSFs using proposed approach.

which can be viewed as the latent ones convolved by a common, hidden, and spurious kernel. A refinement step based on the PSF sparsity and positivity properties is then carried out to *deconvolve the estimated PSFs*. Finally the

output image is computed through a standard non-blind multichannel deconvolution procedure. ALM and IRLS are implemented to efficiently optimize the cost functions involved in this system.

Another possible way of removing the spurious kernel is by adding a PSF sparsity constraint into the preliminary multichannel PSF estimation function (10) directly. We tried such method but the results were not good. Due to the complexity of the objective function with so many constraints on images and kernels, the resulting algorithm can become tangled in local minima, or fail to converge. However, experiments on both simulated and real image sets illustrate that the proposed strategy of post refinement on PSF estimation can efficiently reduce the PSF blur, mitigating the estimation sensitivity to noise and PSF size. Future work involves extending this approach to spatially variant blur.

References

1. Levin, A., Weiss, Y., Durand, F., Freeman, W.T.: Understanding and evaluating blind deconvolution algorithms. CVPR (2009)
2. Shan, Q., Jia, J., Agarwala, A.: High-quality motion deblurring from a single image. ACM Transactions on Graphics (SIGGRAPH) (2008)
3. Levin, A., Fergus, R., Durand, F., Freeman, W.T.: Image and depth from a conventional camera with a coded aperture. ACM Transactions on Graphics (SIGGRAPH) (2007)
4. Joshi, N., Szeliski, R., Kriegman, D.: PSF estimation using sharp edge prediction. CVPR (2008)
5. Cho, T.S., Paris, S., Horn, B.K.P., Freeman, W.T.: Blur kernel estimation using the Radon transform. CVPR (2011)
6. Li, W., Zhang, J., Dai, Q.: Exploring aligned complementary image prior for blind motion deblurring. CVPR (2011)
7. Harikumar, G., Bresler, Y.: Perfect blind restoration of images blurred by multiple filters: Theory and efficient algorithms. IEEE Transactions on Image Processing **8** 202–219 (1999)
8. Giannakis, G.B., Heath, R.W.: Blind identification of multichannel FIR blurs and perfect image restoration. IEEE Transactions on Image Processing **9** 1877–1896 (2000)
9. Rav-Acha, A., Peleg, S.: Two motion-blurred images are better than one. Pattern Recognition Letters **26** 311–317 (2005)
10. Šroubek, F., Milanfar, P.: Robust multichannel blind deconvolution via fast alternating minimization. (Accepted for IEEE Transactions on Image Processing, 10.1109/TIP.2011.2175740)
11. Rudin, L., Osher, S., Fatemi, E.: Nonlinear total variation based noise removal algorithms. Phys. D **60** 259–268 (1992)
12. Xu, L., Jia, J.: Two-phase kernel estimation for robust motion deblurring. ECCV (2010)
13. Levin, A., Weiss, Y., Durand, F., Freeman, W.T.: Exploring aligned complementary image prior for blind motion deblurring. CVPR (2011)
14. Chen, J., Yuan, L., Tang, C., Quan, L.: Robust dual motion deblurring. CVPR (2008)